THE ASTROPHYSICAL JOURNAL, 458:508–513, 1996 February 20

RELATIVISTIC ACCRETION DISKS: LOW-FREQUENCY MODES AND FRAME DRAGGING

JAMES R. IPSER
Department of Physics, University of Florida, Gainesville, FL 32611; ipser@possum.phys.ulf.edu
Received 1995 June 5; accepted 1995 August 25

ABSTRACT

A recently developed formalism is employed to study modes of pulsation of relativistic accretion disks around Kerr black holes. In the present study the disk's self-gravity is neglected, and attention is focused on the existence of modes with very low frequencies and their possible connection with the QPO phenomena exhibited by certain black hole candidates. A by-product is the first available comparison of relativistic and pseudo-Newtonian results. The analyses reveal that in many cases thin relativistic disks exhibit warped tilt/precession modes with frequencies of the order of those associated with QPO phenomena. In the limit of a nonrotating black hole, the modes are all retrograde relative to the disk, with the relativistic frequencies smaller than the corresponding pseudo-Newtonian frequencies by about a factor of 2, due to redshift effects. This correspondence breaks down completely, however, as the black hole is spun up in the direction of disk rotation, due to effects associated with the relativistic phenomenon of the dragging of inertial frames. As the black hole is spun up, frame dragging influences the modes to an unprecedented degree, successively pulling modes through zero frequency so that they become prograde. For disk temperatures appropriate to X-ray emission, frame-dragging effects are dominant even for very small amounts of rotation. These effects allow an explanation in terms of a common mechanism for the full range of observed QPO frequencies ($\sim$0.01–10 Hz).

Subject headings: accretion, accretion disks — black hole physics — relativity

1. INTRODUCTION

An astrophysical problem of considerable interest focuses on the origin of the low frequency quasi-periodic oscillations (QPOs) associated with certain low-mass X-ray binaries and black hole–candidate systems (see, for example, the reviews by Lewin & Tanaka 1994 and by van der Kliss 1989, 1994). In systems containing a black hole, the absence of a magnetic field around the black hole precludes an explanation of the QPO phenomenon in terms of the beat frequency model (Alpar & Shaham 1985). This is partly responsible for a surge of interest in the possibility that, at least in black hole systems, the QPOs are associated with modes of oscillation of an accretion disk.

In an attempt to interpret long-timescale X-ray variability of certain sytems along these lines, several studies have examined the possibility that the QPOs of black hole systems are associated with low-frequency modes trapped in the inner regions of thin accretion disks surrounding the black holes (Kato 1989; Kato & Honma 1991; Ipser 1994). The first two studies worked in the approximation that the disk is vertically isothermal and oscillates without disturbing its temperature distribution. The third study employed a formalism that enables one to treat the general adiabatic perturbations of rotating fluid configurations (Ipser & Lindblom 1991). That study was able to allow for nonadiabatic temperature gradients in the equilibrium disk structure, and it showed that nonadiabatic gradients are unimportant for the low-frequency modes of interest.

The above studies demonstrated that a variety of thin disk models, with sufficiently large pressure gradients in their inner regions, do exhibit low-frequency nonaxisymmetric modes that are trapped in the inner disk regions where the accretion binding energy is liberated. This leads to the suggestion of an association with the QPO phenomenon.

One problem with all of these studies is that they adopt the pseudo-Newtonian approximation, involving of the Newtonian gravitational potential in order to simulate certain general relativistic effects, especially the instability of circular orbits at sufficiently small radii. The purpose of the present paper is to present a general relativistic treatment of the problem under consideration. Such a treatment is now possible because of the development of a formalism for analyzing adiabatic pulsations of rotating relativistic fluids (Ipser & Lindblom 1992; henceforth Paper I). It will be shown that relativistic effects, especially those associated with the dragging of inertial frames in rotating systems, can have profound effects on observable features of the modes, and may in fact help to explain the wide range of frequencies that have been associated with QPOs in black hole–candidate systems.

2. EQUILIBRIUM DISK

The underlying equilibrium structure is that of a geometrically thin axisymmetric disk, composed of perfect fluid that rotates in the axisymmetric gravitational field of a central compact object. The disk is assumed to lie in the equatorial plane. The disk fluid is described by a stress-energy tensor ($G = c = 1$ throughout)

$$T^{ab} = \rho u^a u^b + p q^{ab} , \tag{1}$$

where ρ is the energy density, p is the pressure and u^a is the fluid unit four-velocity. Also, the projection operator q^{ab} is given by

$$q^{ab} = g^{ab} + u^a u^b , \tag{2}$$

where g^{ab} is the inverse of the metric g_{ab}. The fluid four-velocity is taken to be of the form

$$u^a = \gamma(t^a + \Omega\varphi^a) , \tag{3}$$

where t^a and φ^a are the Killing vectors associated with the stationary and rotational symmetries of the spacetime. The scalar γ is a redshift factor and Ω is the fluid angular velocity. In the Cowling approximation, which is adopted here, the

gravitational field is completely determined by the central compact axisymmetric object. The contribution of the disk is neglected, even when it pulsates. Further, in a first approximation, the radial component of the equilibrium velocity, turbulence, and magnetic fields are all neglected.

The gravitational field of the central axisymmetric object is conveniently written in the Bardeen-Wagoner (1971) form

$$ds^2 = g_{ab}\,dx^a\,dx^b = -e^{2\nu}\,dt^2 + B^2e^{-2\nu}\varpi^2(d\varphi - \alpha dt)^2 + e^{2(\zeta-\nu)}(d\varpi^2 + dz^2)\,. \tag{4}$$

Here the metric functions ν, B, α, ζ are functions of the cylindrical coordinates ϖ and z, and t and φ are the time and angular coordinates associated with the Killing vectors.

The assumption of a thin disk allows one to expand equations in powers of z/ϖ and keep only the lowest order terms. As a result, it becomes convenient to work with the Kepler angular velocity $\Omega_K(\varpi)$ of a geodesic circular orbit in the equatorial plane of the central object. This quantity satisfies the equation

$$g_{tt,\varpi} + 2g_{t\varphi,\varpi}\Omega_K + g_{\varphi\varphi,\varpi}\Omega_K^2 = 0 \tag{5}$$

evaluated at $z = 0$. Throughout this paper a comma denotes a partial derivative, while ∇_a denotes the covariant derivative. In terms of Ω_K, the radial component of the equilibrium Euler equation $q_{ab}\nabla_c T^{bc} = 0$ takes the form

$$\frac{\rho_{,\varpi}}{\rho + p} = \frac{p_{,\varpi}}{c_s^2(\rho + p)} = \frac{1}{2}\frac{\gamma^2}{c_s^2}\left[(\Omega_K^2 - \Omega^2)g_{\varphi\varphi,\varpi} + 2(\Omega_K - \Omega)g_{t\varphi,\varpi}\right], \tag{6a}$$

while the axial component is

$$\frac{\rho_{,z}}{\rho + p} = \frac{p_{,z}}{c_s^2(\rho + p)} = \frac{\gamma^2}{2c_s^2}\left(g_{tt,z} + 2\Omega g_{t\varphi,z} + \Omega^2_{g_{\varphi\varphi,z}}\right) \equiv -\gamma^2 e^{2(\zeta-\nu)}\frac{\Omega_p^2}{c_s^2}\,z\,. \tag{6b}$$

The quantity Ω_p is the angular velocity of vertical oscillations, perpendicular to the disk plane, exhibited by a particle perturbed vertically from a geodesic circular orbit. When the central object is spherically symmetric, $\Omega_p = \Omega_K$, but frame-dragging effects break this symmetry in the rotating case, where $\Omega_p < \Omega_K$. It will become evident that this symmetry breaking plays a key role in determining the frequencies of the pulsation modes that are studied in this paper. The angular velocity Ω_p and the other coefficients in equation (6) are evaluated at $z = 0$ in the thin-disk approximation. The above equations determine the equilibrium structure once the pressure-density relation and the angular velocity Ω are specified. In this connection, the integrability condition for equation (6) is that $\Omega = \Omega(\gamma u_a \varphi^a)$.

3. ADIABATIC PULSATIONS OF THE DISK

We employ the formalism of Paper I, which provides the tools needed for analyzing the general adiabatic modes of pulsation of rotating relativistic fluids in the Cowling approximation. In this first application we shall confine attention to barotropic configurations, in which the pressure and energy density are unique functions of one another. This considerably reduces the complexity of the equations.

3.1. *Covariant Form of the Eigenequation*

The formalism is applicable to normal mode pulsations with time and angular dependences of the form $e^{i\omega t + im\varphi}$, where ω is the angular frequency of oscillation and m is the azimuthal angular index. The formalism reveals that the hydrodynamical degrees of freedom of adiabatic pulsations of relativistic fluids are described by a single scalar potential that satisfies an eigenequation with ω as eigenvalue. In the barotropic case, where $p = p(\rho)$, the vector A^a defined by Paper I, equation (18), vanishes. As a result, the pulsation equation (Paper I, eq. [39]) reduces to

$$\frac{1}{\varpi^*}D_a\left[\frac{\varpi^*\Lambda}{\sigma^2\gamma^2}(\rho + p)(\sigma^2\gamma^2 h^{ab} - 2\omega^a\Omega^b)D_b\,\delta V\right] + \sigma\gamma\Phi\,\delta V = 0\,. \tag{7}$$

Here h^{ab} is the inverse of h_{ab}, the metric on the $\varpi - z$ plane, and D_a is the associated covariant derivative. The rotating-frame angular velocity $\sigma = \omega + m\Omega$, and $\varpi^{*2} \equiv q_{ab}\varphi^a\varphi^b/\gamma^2 = (\varpi B)^2$ in Bardeen-Wagoner coordinates. The vorticity ω^a and the angular velocity vector Ω^a satisfy (see Paper I, eqs. [22] and [23])

$$\omega^a = 2\Omega^a + \epsilon^{ab}\gamma^2\varpi^* D_b\,\Omega = \frac{\epsilon^{ab}}{\gamma^2\varpi^*}\left[D_b(\gamma u_c\,\varphi^c) - (\gamma u_c\,\varphi^c)D_b\,\Omega\right], \tag{8}$$

where the antisymmetric tensor ϵ^{ab} is the volume element on the $\varpi - z$ two-surface. These quantities determine Λ through the relation $\Lambda = \sigma^2\gamma^2/(\sigma^2\gamma^2 - 2\omega^a\Omega_a)$. Further, Φ is defined by (see Paper I, eqs. [31], [41], [42])

$$\Phi = \frac{\sigma\gamma}{c_s^2}(\rho + p) + H^a D_a\,p - \frac{1}{\varpi^*}D_a[\varpi^*(\rho + p)H^a] + \frac{1}{\varpi^*}D_a\left[\frac{\varpi^*}{\sigma^2\gamma^2}(\rho + p)H^{ab}D_b(\sigma\gamma)\right] - \frac{\Lambda(\rho + p)}{\varpi^{*2}\sigma\gamma^3}(m + \sigma\gamma u_a\,\varphi^a)^2\,, \tag{9}$$

where $c_s = (dp/d\rho)^{1/2}$, the speed of sound, and

$$H^{ab} = \frac{\Lambda}{\sigma^2\gamma^2}(\sigma^2\gamma^2 h^{ab} - 2\omega^a\Omega^b)\,, \qquad H^a = \frac{2\Lambda}{\varpi^*\sigma^2\gamma^3}(m + \sigma\gamma u_b\,\varphi^b)\epsilon^{ac}\Omega_c\,. \tag{10}$$

The eigenfunction δV in equation (7) is defined by

$$\delta V = \frac{\delta p}{\sigma\gamma(\rho + p)}\,, \tag{11}$$

where δp is the Eulerian perturbation of the pressure.

3.2. *An Approximate Eigenequation in Bardeen-Wagoner Coordinates*

We are interested here in the modes of thin disks for which $c_s^2 \sim (z/\varpi)^2 \ll 1$. Hence it is appropriate to expand the eigenequation formally in powers of c_s^2 and to keep only the lowest order, dominant terms. Recalling that $\Omega = \Omega(\gamma u_a \varphi^a)$, we first introduce new orthogonal coordinates $\bar{z}, \bar{\varpi}$ such that

$$\bar{\varpi} = f(\gamma u_a \varphi^a) = \varpi[1 + \mathcal{O}(z^2/\varpi^2)] ,$$
$$\bar{z} = z[1 + \mathcal{O}(z^2/\varpi^2)] , \tag{12}$$

and hence such that $\Omega = \Omega(\bar{\varpi})$ and $\omega^{\bar{\varpi}} = \Omega^{\bar{\varpi}} = 0$. In terms of the barred coordinates, the eigenequation (7) becomes

$$\frac{1}{\varpi^* \sqrt{^2g}} \frac{\partial}{\partial \bar{z}} [\varpi^* \sqrt{^2g}(\rho + p) g^{\bar{z}\bar{z}} \delta V_{,\bar{z}}] + \frac{1}{\varpi^* \sqrt{^2g}} \frac{\partial}{\partial \bar{\varpi}}$$
$$\times \left[\frac{\varpi^* \sqrt{^2g}(\rho + p)\sigma^2 \gamma^2 g^{\bar{\varpi}\bar{\varpi}}}{(\sigma^2\gamma^2 - 2\omega^{\bar{z}}\Omega_{\bar{z}})} \delta V_{,\bar{\varpi}} \right] + \sigma\gamma\Phi\, \delta V = 0 . \tag{13}$$

We next expand formally in powers of c_s^2. Using the equilibrium equation (6), we then obtain, at lowest order in c_s^2,

$$\frac{\partial}{\partial z}\left(\rho \frac{\partial \delta V}{\partial z}\right) + \frac{\sigma^2}{(\sigma^2 - \kappa^2)} \frac{\partial}{\partial \varpi}\left(\rho \frac{\partial \delta V}{\partial \varpi}\right)$$
$$+ \left\{ e^{2(\zeta - \nu)} \frac{\sigma^2 \gamma^2 \rho}{c_s^2} + \left[\frac{\sigma\gamma \mathscr{F}}{\varpi B} + \frac{\Lambda(\sigma\gamma)_{,\varpi}}{\sigma\gamma} \right] \rho_{,\varpi} \right\} \delta V \approx 0 . \tag{14}$$

In this equation, it is consistent to neglect the z-dependence of all coefficients once the derivatives of ρ have been evaluated by using equation (6). Hence the barred coordinates have been replaced by the Bardeen-Wagoner coordinates. Further

$$\mathscr{F} \equiv \frac{\Lambda(m + \sigma S)}{\sigma^2 \gamma^5 \varpi B} [S_{,\varpi} - S^2 \Omega_{,\varpi} - (\gamma \varpi B)^2 \Omega_{,\varpi}] , \tag{15}$$

$$2\omega^z \Omega_z \equiv \kappa^2 \gamma^2$$
$$= \frac{e^{-2(\zeta - \nu)}}{\gamma^4 \varpi^2 B^2} (S_{,\varpi} - S^2 \Omega_{,\varpi})^2 - e^{-2(\zeta - \nu)} (S_{,\varpi} - S^2 \Omega_{,\varpi}) \Omega_{,\varpi} , \tag{16}$$

where

$$S \equiv \gamma u_\varphi = \frac{e^{-4\nu} B^2 \varpi^2 (\Omega - \alpha)}{1 - e^{-4\nu} B^2 \varpi^2 (\Omega - \alpha)^2} , \tag{17}$$

and

$$\gamma = e^{-\nu}[1 + (\Omega - \alpha) S]^{1/2} . \tag{18}$$

The quantity κ is the relativistic epicyclic frequency associated with radial perturbations of geodesic circular orbits in the equatorial plane.

3.3. *An Approximate Dispersion Relation*

Equation (14) admits an approximation relativistic dispersion relation that can be compared with its nonrelativistic analogs (see, e.g. Kato 1989; Ipser 1994). Equation (6b) suggests that the effective wave number in the z direction is $\sim \gamma e^{\zeta - \nu} \Omega_p / c_s$. If $e^{\zeta - \nu} k_\varpi$ denotes the effective radial wave number, then equation (14) implies the local dispersion relation

$$(\sigma^2 - \kappa^2)(\sigma^2 - \Omega_p^2 + \tilde{f}) \approx \sigma^2 c_s^2 k_\varpi^2 / \gamma^2 , \tag{19}$$

where $\tilde{f}$ is a multiple of the coefficient of $\rho_{,\varpi} \delta V$ in equation (14). This dispersion relation suggests that when $|\Omega_K - \Omega_p| \sim |\Omega_K - \Omega| \ll \Omega$, low-frequency ($\omega \ll \Omega$)$m = 1$ modes exist and satisfy

$$\omega \approx -\frac{(\Omega_K - \Omega_p)(\Omega + \Omega_p)}{2\Omega} + \frac{(\Omega_K - \Omega)(\Omega + \Omega_p)}{2\Omega}$$
$$- \frac{\tilde{f}}{2\Omega} + \frac{\Omega c_s^2 k_\varpi^2}{2(\Omega^2 - \kappa^2)\gamma^2} . \tag{20}$$

This expression suggests that any increase in $(\Omega_K - \Omega_p)$ due to frame dragging will lead to a decrease in ω. We will return to this possibility later.

4. WARPED PRECESSION MODES OF RELATIVISTIC DISKS

4.1. *The Radial Eigenequation and Its Boundary Condition*

As in the pseudo-Newtonian problem, we shall research for low-frequency modes with $m = 1$ and with eigenfunctions of the form

$$\delta V(z, \varpi) \approx z F(\varpi) . \tag{21}$$

These modes describe situations in which a disk tilts, warps, and precesses about the rotation axis. In these cases, equations (6b) and (14) yield the radial eigenequation

$$\frac{d}{d\varpi}\left(\rho^* \frac{dF}{d\varpi}\right) + \frac{(\sigma^2 - \kappa^2)}{\sigma^2}$$
$$\left\{ e^{2(\zeta - \nu)}(\sigma^2 - \Omega_p^2) \frac{\gamma^2 \rho^*}{c_s^2} + \left[\frac{\sigma\gamma \mathscr{F}}{\varpi B} + \frac{\Lambda(\sigma\gamma)_{,\varpi}}{\sigma\gamma} \right] \rho^*_{,\varpi} \right\} F \approx 0 , \tag{22}$$

where

$$\rho = \rho^*(\varpi) e^{-z^{*2}/2} , \quad z^* \equiv z/H_z , \quad H_z \equiv e^{-(\zeta - \nu)} c_s / (\Omega_p \gamma) . \tag{23}$$

We are interested in modes that are trapped, or confined, within the inner regions of the disk. Hence we impose the outer boundary condition that physical perturbation quantities, such as the local energy density of pulsation, die out in the outer regions of the disk. Since the local energy density of pulsation is roughly proportional to ρF^2, it is convenient to make a change of dependent variable in equation (22) to $\rho^{*1/2} F$, which also has the effect of eliminating the first-derivative term. We can then impose the outer boundary condition by demanding that $\rho^{*1/2} F$ dies out, approximately exponentially it turns out, at large ϖ. We impose the inner boundary condition that $F = 0$ at the inner edge of the disk, which we take to lie at the last stable circular orbit. This is generally required in order to guarantee that the Lagrangian perturbation of the pressure vanishes at the inner edge of the disk for our choices of the angular velocity $\Omega(\varpi)$.

4.2. *Application to the Kerr Geometry*

In the remainder of this paper we focus on disks around Kerr black holes. In the usual Boyer-Lindquist coordinates the

Kerr geometry is (Chandrasekhar 1983)

$$ds^2 = -\frac{R^2\Delta}{\Sigma^2}\,dt^2 + \frac{\Sigma^2}{R^2}\sin^2\theta\left(d\varphi - \frac{2aMr_{\rm BL}}{\Sigma^2}\,dt\right)^2 + \frac{R^2}{\Delta}\,dr_{\rm BL}^2 + R^2\,d\theta^2\,, \tag{24}$$

where M is the black hole mass, a is the usual Kerr parameter = (angular momentum)/mass, and where

$$\Delta = r_{\rm BL}^2 - 2Mr_{\rm BL} + a^2\,, \quad R^2 = r_{\rm BL}^2 + a^2\cos^2\theta\,,$$
$$\Sigma^2 = (r_{\rm BL}^2 + a^2)^2 - a^2\Delta\sin^2\theta\,. \tag{25}$$

The connection between the Boyer-Lindquist radial coordinate $r_{\rm BL}$ and the Bardeen-Wagoner coordinates is given by

$$r_{\rm BL} = [(2r + M)^2 - a^2]/4r\,, \quad r \equiv (\varpi^2 + z^2)^{1/2}\,. \tag{26}$$

It is easily verified that the Bardeen-Wagoner metric functions for the Kerr geometry take the forms

$$e^{2\nu} = R^2\Delta/\Sigma^2\,, \quad B^2 = \Delta/(\varpi^2 + z^2)\,,$$
$$\alpha = 2aMr_{\rm BL}/\Sigma^2\,, \quad e^{2(\zeta-\nu)} = R^2/(\varpi^2 + z^2)\,. \tag{27}$$

Further, the radius $r_{\rm BL,min}$ of the last stable circular orbit, where the inner edges of our disks lie, satisfies the equation (Chandrasekhar 1983)

$$r_{\rm BL,min}^2 - 6r_{\rm BL,min} + 8ar_{\rm BL,min}^{1/2} - 3a^2 = 0\,. \tag{28}$$

5. RESULTS AND DISCUSSION

In this paper we study relativistic disks with constant thickness H_z (eq. [23]) and with rotation laws of the form

$$\Omega^2 = \Omega_{\rm K}^2\left[1 - \frac{\beta}{2M^2}(r_{\rm BL} - r_{\rm BL,min})(r_{\rm BL} - r_2)(r_{\rm BL}/r_2)^{-4}\right], \tag{29}$$

where β and r_2 are constants. This form is the relativistic analogue of the form used in earlier pseudo-Newtonian calculations. This permits study of the extent to which properties of pseudo-Newtonian disks can mimic those of relativistic disks. When using the rotation law (29), one should guarantee that β is large compared with c_s^2. Otherwise the expansion in powers of c_s^2 that leads to equation (14) will break down. We will confine attention to disks with $\beta/c_s^2 \gtrsim 10$. Fortunately, it is precisely the larger values of β that do admit trapped modes of the kind sought.

A first comparison of relativistic and pseudo-Newtonian disks is provided by Table 1, which exhibits the frequencies of certain pseudo-Newtonian trapped modes and of the corresponding relativistic modes in the spherical black hole limit ($a = 0$) for $c_s = 10^{-3}$ at the inner edge of the accretion disk. The first two columns define the rotation law (29). The column label N denotes the number of nodes in the radial eigenfunction F. The label $r_E/2M$ denotes the approximate radius, or value of ϖ in the equatorial plane, at which a mode begins to die out exponentially. The unit $2M$ is twice the mass of the central black hole. The last two columns exhibit the frequencies $f = \omega/2\pi$ of relativistic modes for a nonrotating black hole and of the corresponding pseudo-Newtonian modes. The frequencies in these cases are all positive, corresponding to modes that are retrograde (points with a given magnitude of displacement, say, rotate in the direction opposite to the direction of disk rotation). Further, it is evident that in the limit of a nonrotating central source, the relativistic frequencies of these warped precession modes are consistently smaller than their pseudo-Newtonian counterparts by about a factor of 2. This difference can be attributed to redshift effects, which are neglected in the pseudo-Newtonian approximation. In most other ways, the pseudo-Newtonian results mimic fairly well the relativistic results for nonrotating holes.

This correspondence in the nonrotating limit is somewhat misleading, however. Significant differences, associated with the dragging of inertial frames, emerge when the central black hole is allowed to rotate. Evidence that frame-dragging effects can strongly affect the frequencies of the modes under consideration is provided by the form (eq. [20]) of the dispersion relation derived earlier. When the central black hole rotates in the same direction as the disk, as is assumed here, one finds that the quantity $(\Omega_{\rm K} - \Omega_p)/\Omega_{\rm K}$ increases as the Kerr parameter increases. This is because the perpendicular oscillation frequency Ω_p of an orbiting particle is given roughly by the rotation rate as sensed locally; and, due to frame-dragging effects, that local rate becomes progressively less than the rate

TABLE 1

CORRESPONDING FREQUENCIES OF PSEUDO-NEWTONIAN AND RELATIVISTIC MODES ($a = 0$)

				$f(M/M_\odot)$ (Hz)	
$r_2/2M$	$\beta/c_{s,\rm in}^2$	N	$r_E/2M$	Relativistic ($a = 0$)	Pseudo-Newtonian
3.5.....	100	1	4	0.46	0.92
3.5.....	100	2	4.5	0.94	1.9
3.5.....	10			No trapped mode	
4.5.....	100	1	5	0.96	1.8
4.5.....	100	2	5	1.8	3.6
4.5.....	10	1	5.5	0.086	0.18
4.5.....	10	2	6	0.18	0.34
5.0.....	100	1	5.5	1.3	2.5

NOTE.—The column labels are defined in the text. The speed of sound has the value $c_{s,\rm in} = 10^{-3}$ at the inner edge of the disk. The central black hole is nonrotating.

Ω_K seen at infinity, as the hole spins up. Hence, from equation (20), one expects that frame-dragging should decrease ω below its nonrotating-limit value by an amount $\bar{\delta}\omega$ satisfying

$$\frac{\bar{\delta}\omega}{2\pi}\frac{M}{M_\odot} \sim \frac{-2aM}{r^3}\frac{M/M_\odot}{2\pi} \sim -10^2\frac{a}{M}\ \text{Hz}\,. \qquad (30)$$

According to equation (30), frame-dragging effects, even for small amounts of rotation, can decrease mode frequencies by large percentages, and can even drag modes through zero frequency so that they become prograde. Figure 1 shows that this is exactly what happens for the value $c_{s,\text{in}} = 10^{-3}$, where $c_{s,\text{in}}$ is the value of the speed of sound at the inner edge of the accretion disk. Figure 1 exhibits the lowest three modes associated with the rotation law parameters $r_2/2M = 3.5$, $\beta/c_{s,\text{in}}^2 = 10^2$. These modes have one, two, and three nodes, respectively. We note, in this connection, that we did not find any trapped modes with zero nodes. Figure 1 reveals that the lowest mode is dragged through zero frequency, and becomes prograde, at $a/M \approx 0.005$, which is in good agreement with the order-of-magnitude estimate provided by equation (30). Figure 1 also indicates that another mode is dragged through zero frequency for each increase of a/M by an amount ~ 0.005. Indeed one finds that for disk temperatures appropriate to X-ray emission, typically more than a hundred modes are dragged from retrograde to prograde, and all existing modes are prograde for $a/M \gtrsim 0.6$. For the case $c_{s,\text{in}} = 10^{-3}$, $r_2/2M = 3.5$ and $\beta/c_{s,\text{in}}^2 = 10^2$, this is demonstrated in Figure 2, which exhibits the frequency of the highest existing mode (modes with largest number of nodes and largest frequency, including sign). The highest mode becomes prograde at $a/M \approx 0.55$. Hence for all smaller values of a/M there is a mode quite close to zero frequency.

The values of a/M at which the lowest modes pass through zero frequency can be pushed to somewhat larger values by increasing $\beta/c_{s,\text{in}}^2$ and/or $c_{s,\text{in}}^2$. This is evident from Figure 3, which exhibits the frequencies of the lowest three modes in a very hot disk with $c_{s,\text{in}} = 10^{-2}$, $r_2/2M = 3.5$, $\beta/c_{s,\text{in}}^2 = 3 \times 10^2$. In this case the lowest three modes pass through zero frequency at $a/M \approx 0.3$, 0.4, and 0.5, respectively.

The above results provide evidence that relativistic accretion disks around black holes can support warped precession

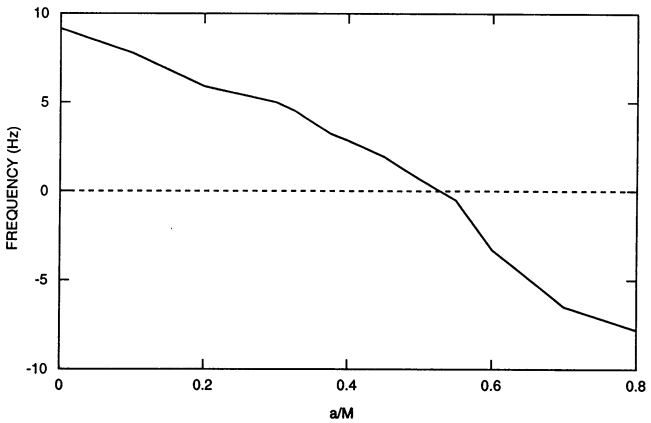

FIG. 2.—The mode with the largest frequency, including sign, for the disk of Figure 1. The vertical scale is the frequency in Hz multiplied by the black hole mass in units of a solar mass.

modes with very low frequencies. For black holes of the order of a solar mass with disk temperature of the order of 10^7 K, the frequencies range from the order of 10 Hz down to 0. The frequencies scale like the inverse of the black hole mass and are approximately proportional to the square of the speed of sound and to the temperature. Frequencies arbitrarily close to zero can be obtained in principle, due to effects associated with the dragging of inertial frames. Hence whether the frequencies are relatively high, as in the case of the 6 Hz QPOs observed in the power spectra of GX 339−4 (Miyamoto, Kimura, & Kitamoto 1991), or low, as in the case of the 0.04 Hz QPOs observed in Cyg X−1 (Vikhlinin et al. 1994) and in the case of GRO J0422 + 32 (Pietsch et al. 1993), the presence of frame dragging allows an explanation in terms of a common mechanism.

If one is unconcerned with the number of nodes of a mode, the problem of constructuring a model with a mode frequency arbitrarily close to zero is not a fine-tuning problem. This is because slight adjustments of the rotation law will yield a zero-frequency mode for any value of $a/M \lesssim 0.6$ in the case of an X-ray–emitting disk. However, if the modes with at most a few nodes are preferentially selected for excitation, then, unless the

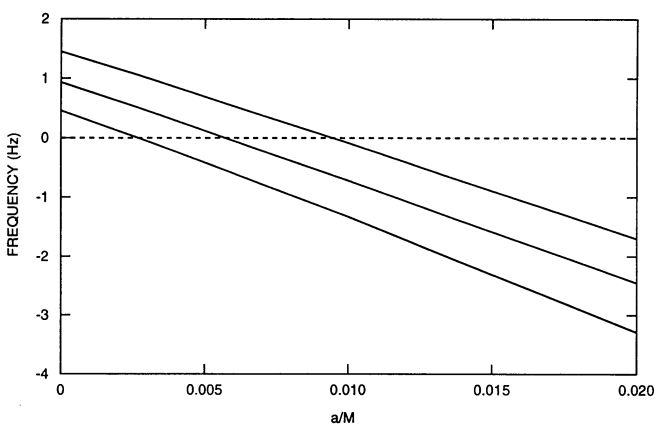

FIG. 1.—The lowest three modes of a disk with $c_{s,\text{in}} = 10^{-3}$ (value of speed of sound at inner edge of disk) and with parameter values $r_2/2M = 3.5$, $\beta/c_{s,\text{in}}^2 = 10^2$ in eq. (29). The vertical scale is the frequency in Hz multiplied by the black hole mass in units of a solar mass.

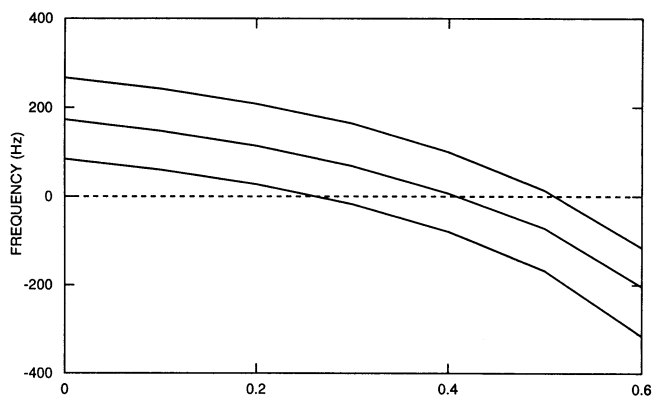

FIG. 3.—The lowest three modes of a disk with $c_{s,\text{in}} = 10^{-2}$, $r_2/2M = 3.5$, $\beta/c_{s,\text{in}}^2 = 3 \times 10^2$. The vertical scale is the frequency in Hz multiplied by the black hole mass in units of a solar mass.

black hole mass is rather large, excited modes can be expected to exhibit frequencies as small as a fraction of Hz only for $a/M \ll 0.1$. In such a case the QPO phenomenon would probably not be associated with rapidly rotating black holes.

In any event, our results lend some support to the interesting possibility that warped precession modes of relativistic accretion disks provide the source of the QPO phenomena associated with presumed black holes. This possibility is especially exciting for the relativist, since it involves a phenomenon in which the dragging of inertial frames can play a strong and vital role. It will be important, in this context, to investigate in detail the way in which warped precession modes can modulate disk emissions and the extent to which they are affected by the accretion process, viscous effects, and the disk's self-gravity.

It is a pleasure to thank Lee Lindblom for crucial and illuminating suggestions. This work was supported in part by NSF grant PHY-9408910.

REFERENCES

Alpar, M. A., & Shaham, J. 1985, Nature, 316, 239
Bardeen, J. M., & Wagoner, R. V. 1971, ApJ, 167, 359
Chandrasekhar, S. 1983, The Mathematical Theory of Black Holes (Oxford: Clarendon Press)
Ipser, J. R. 1994, ApJ, 435, 767
Ipser, J. R., & Lindblom, L. 1991, ApJ, 379, 285
———. 1992, ApJ, 389, 392 (Paper I)
Kato, S. 1989, PASJ, 41, 745
Kato, S., & Honma, F. 1991, PASJ, 43, 95
Lewin, W. H. G., & Tanaka, Y. 1994, in X-Ray Binaries, ed. W. H. G. Lewin, J. van Paradijs, & E. P. J. van den Heuvel (Cambridge: Cambridge Univ. Press)
Miyamoto, S., Kimura, K., & Kitamoto, S. 1991, ApJ, 383, 784
Pietsch, W., Harberl, F., Gehrels, N., & Petre, R. 1993, A&A, 273, L11
van der Klis, M. 1989, ARA&A, 27, 517
———. 1994, in X-Ray Binaries, ed. W. H. G. Lewin, J. van Paradijs, & E. P. J. van den Heuvel (Cambridge: Cambridge Univ. Press)
Vikhlinin, A., et al. 1994, ApJ, 424, 395